



RESEARCH PAPER

Greater aperture counteracts effects of reduced stomatal density on water use efficiency: a case study on sugarcane and meta-analysis

Daniel Lunn^{1,2,3,4, }, Baskaran Kannan^{5,6, }, Amandine Germon^{1,2,†, }, Alistair Leverett^{1,2,§, }, Tom E. Clemente^{7,8, }, Fredy Altpeter^{5,6, }, and Andrew D. B. Leakey^{1,2,3,4,9,*, }

¹ Carl R. Woese, Institute of Genomic Biology, 1206 W. Gregory Drive, University of Illinois Urbana-Champaign, Urbana, IL 61801, USA

² Center for Advanced Bioenergy and Bioproducts Innovation, 1206 W. Gregory Drive, University of Illinois Urbana-Champaign, Urbana, IL 61801, USA

³ Department of Plant Biology, University of Illinois Urbana-Champaign, Urbana, IL 61801, USA

⁴ Center for Digital Agriculture, University of Illinois Urbana-Champaign, Urbana, IL 61801, USA

⁵ Agronomy Department, 3105 McCarty Hall B, University of Florida, Gainesville, FL 32603, USA

⁶ Center for Advanced Bioenergy and Bioproducts Innovation, 3105 McCarty Hall B, University of Florida, Gainesville, FL 32603, USA

⁷ Department of Agronomy and Horticulture, 202 Keim Hall, University of Nebraska-Lincoln, Lincoln, NE 68583, USA

⁸ Center for Advanced Bioenergy and Bioproducts Innovation, 202 Keim Hall, University of Nebraska-Lincoln, Lincoln, NE 68583, USA

⁹ Department of Crop Sciences, University of Illinois Urbana-Champaign, Urbana, IL 61801, USA

† Present address: UMR Eco&Sols, Univ Montpellier, CIRAD, INRAE, IRD, InstitutAgro Montpellier, Montpellier, France.

‡ Present address: CIRAD, UMR Eco&Sols, Montpellier F-34398, France.

§ Present address: Department of Plant Science, University of Cambridge, Downing Street, Cambridge CB2 3EA, UK.

* Correspondence: leakey@illinois.edu

Received 9 February 2024; Editorial decision 28 May 2024; Accepted 17 July 2024

Editor: John Lunn, MPI of Molecular Plant Physiology, Germany

Abstract

Stomata regulate CO₂ and water vapor exchange between leaves and the atmosphere. Stomata are a target for engineering to improve crop intrinsic water use efficiency (iWUE). One example is by expressing genes that lower stomatal density (SD) and reduce stomatal conductance (g_{sw}). However, the quantitative relationship between reduced SD, g_{sw} , and the mechanisms underlying it is poorly understood. We addressed this knowledge gap using low-SD sugarcane (*Saccharum* spp. hybrid) as a case study alongside a meta-analysis of data from 10 species. Transgenic expression of EPIDERMAL PATTERNING FACTOR 2 from *Sorghum bicolor* (SbEPF2) in sugarcane reduced SD by 26–38% but did not affect g_{sw} compared with the wild type. Further, no changes occurred in stomatal complex size or proxies for photosynthetic capacity. Measurements of gas exchange at low CO₂ concentrations that promote complete stomatal opening to normalize aperture size between genotypes were combined with modeling of maximum g_{sw} from anatomical data. These data suggest that increased stomatal aperture is the only possible explanation for maintaining g_{sw} when SD is reduced. Meta-analysis across C₃ dicots, C₃ monocots, and C₄ monocots revealed that engineered reductions in SD are strongly correlated with lower g_{sw} ($r^2=0.60–0.98$), but this response is damped relative to the change in anatomy.

Keywords: Epidermal patterning, epidermal patterning factor, stomatal conductance, stomatal density, water use efficiency.

Abbreviations: A_n , net photosynthetic CO₂ assimilation; g_{sw} , stomatal conductance; iWUE, intrinsic water use efficiency; SD, stomatal density.

© The Author(s) 2024. Published by Oxford University Press on behalf of the Society for Experimental Biology.

This is an Open Access article distributed under the terms of the Creative Commons Attribution License (<https://creativecommons.org/licenses/by/4.0/>), which permits unrestricted reuse, distribution, and reproduction in any medium, provided the original work is properly cited.

Introduction

Engineering crops to have greater water use efficiency (WUE) is a key target for crop improvement to deal with the increased frequency and intensity of drought periods resulting from climate change (Leakey *et al.*, 2019). At the leaf level, intrinsic WUE (iWUE) is defined as the ratio of net photosynthetic CO₂ assimilation (A_n) relative to stomatal conductance (g_{sw}). A_n and g_{sw} are generally tightly coupled (Leakey *et al.*, 2019), but if g_{sw} can be reduced with less or no reduction in A_n , it can result in greater iWUE along with lower water use per unit of biomass production at the whole-plant scale (Yoo *et al.*, 2009). The level of g_{sw} is a function of stomatal density (SD), stomatal complex size, and stomatal aperture (Franks *et al.*, 2009). Although any of these parameters could be altered to lower g_{sw} , there is a strong proof-of-concept for reducing SD by manipulating the gene network regulating stomatal development (Harrison *et al.*, 2020).

The ultimate effect of lowering SD will depend on whether changes in stomatal complex size and/or stomatal aperture coincide with amplifying or ameliorating the g_{sw} response. There is broad evidence that both unintended effects can co-occur with the targeted reduction in SD. For example, in Arabidopsis, pepper, poplar, and rice, engineered reductions in SD coincide with greater stomatal complex size (Zhu *et al.*, 2015; Wang *et al.*, 2016; Mohammed *et al.*, 2019; Zhao *et al.*, 2020; Li *et al.*, 2021; Karavolias *et al.*, 2023). However, the opposite response of smaller stomata in low-SD plants has been observed in barley and rice (Hughes *et al.*, 2017; Caine *et al.*, 2019). Overexpression of EPIDERMAL PATTERNING FACTOR 1 (EPF1) or knockout of EPF-Like 9 (EPFL9) increased stomatal complex size in the rice cultivar Nipponbare (Mohammed *et al.*, 2019; Karavolias *et al.*, 2023). Conversely, overexpression of EPF1 in IR64 decreased stomatal size (Caine *et al.*, 2019). In addition, engineered reductions in SD coincided with greater stomatal aperture in Arabidopsis and rice (both Nipponbare and IR64) when that was estimated from epidermal impressions/peels or inferred from increases in the ratio of operating g_{sw} from gas exchange to maximum g_{sw} from anatomical data (Büßis *et al.*, 2006; Franks *et al.*, 2015; Caine *et al.*, 2019; Karavolias *et al.*, 2023). However, the conditions under which these mechanisms ameliorate or enhance the resulting impact on g_{sw} have not been widely tested and are poorly understood. In addition, the quantitative relationship between reduced SD and g_{sw} has not been broadly assessed. This study aims to address this knowledge gap by (i) reducing SD in the C₄ species sugarcane to evaluate interactions between stomatal anatomy and leaf gas exchange fluxes; and (ii) performing a meta-analysis of the relationship between engineered reductions in SD and g_{sw} .

C₄ species are a potentially valuable system for engineering crops with low SD to improve iWUE. As a result of their CO₂-concentrating mechanism and recent increases in atmospheric [CO₂], photosynthesis in C₄ crops is CO₂ saturated (Leakey *et al.*, 2019; Pignon and Long, 2020). Therefore, a moderate

reduction in g_s that reduces intercellular [CO₂] (c_i) to the lowest possible concentration without dropping below the inflection point of the A/c_i curve can lower transpiration and preserve soil moisture to avoid drought stress without increasing stomatal limitation to A_n . The evidence for this comes from (i) leaf-level gas exchange modeling and process-based crop modeling (Leakey *et al.*, 2019; Pignon and Long, 2020); (ii) FACE (free air CO₂ enrichment) experiments where photosynthesis or biomass production was not stimulated when C₄ crops are grown at elevated [CO₂] and with adequate water supply (Leakey *et al.*, 2009; Markelz *et al.*, 2011; Kellner *et al.*, 2019); and (iii) transgenic sorghum and maize with low SD (Liu *et al.*, 2015; Ferguson *et al.*, 2024). In this study, C₄ species are an attractive system because it should be possible to study interactions between g_{sw} , SD, and stomatal complex size as they vary without changes in photosynthetic capacity or A_n . In contrast, photosynthesis in C₃ species under typical growth conditions is sensitive to variations in intracellular CO₂. Thus, reducing g_{sw} in C₃ species lowers c_i , resulting in increased stomatal limitation of A_n (Farquhar and Sharkey, 1982). Most studies of low-SD C₃ plants show this phenomenon, with A_n values lower than the wild type (Hughes *et al.*, 2017; Caine *et al.*, 2019; Dunn *et al.*, 2019; Li *et al.*, 2021; Karavolias *et al.*, 2023). Therefore, since g_{sw} is also tightly coupled to A_n , any potential feedback between the two complicates the interpretation of structure–function relationships.

Some of the mechanisms that may act to modify the effect on g_{sw} from reducing SD are developmental. Overexpression of EPFs is understood to suppress SD via a reduction in stomatal index that results from cells halting progression at multiple stages of stomatal development (Hughes *et al.*, 2017; Caine *et al.*, 2019). However, less is understood about the downstream aspects of engineering low-SD plants on other aspects of epidermal patterning that could impact leaf gas exchange. A recent report showed that increasing SD did not impact bulliform density but increased hair and silica cells (Abrash *et al.*, 2018). These structures should not be overlooked since hair cell types play an important role in boundary layer conductance that can impact gas exchange (Bickford, 2016). Given the significance of stomatal clustering to gas exchange (Dow *et al.*, 2014), important differences could result from whether reduced SD arises due to fewer stomata per cell file and/or fewer files of cells containing stomata on a grass leaf. Signals that impact stomatal development can also modify other epidermal cell types, such as hair cells (Torii, 2021). Alterations in the proportion and development of different cell types may provide feedback on how stomatal complex size is determined. However, despite discovering some genes that regulate stomatal complex size, this process is less well understood than cell fate regulation (Des Marais *et al.*, 2014; Nunes *et al.*, 2020).

The network of genes regulating stomatal development is a model system for studying the regulation of cell fate and

has been extensively elucidated in *Arabidopsis* (Simmons and Bergmann, 2016). The collective function of these genes is largely conserved between C_3 dicots and grasses, but some specifics of individual gene function have diverged (McKown and Bergmann, 2020). The potential for novel function is highlighted by the dumbbell-shaped guard cells flanked by a subsidiary cell that distinguishes grass stomata from the classic kidney-shaped guard cells of dicots (Nunes *et al.*, 2020). Establishing guard cell identity in *Brachypodium* and rice requires transcription factors INDUCER OF CBP EXPRESSION 1 (ICE1) and one active copy of either SPEECHLESS 1 (SPCH1) or SPEECHLESS 2 (SPCH2) (Raissig *et al.*, 2016; Wu *et al.*, 2019). The resulting SPCH:ICE heterodimer stimulates gene expression whereby precursor cells asymmetrically divide to produce a guard mother cell and a pavement cell. Lateral signals then radiate from the guard mother cell to stimulate subsidiary cell formation before a final longitudinal division produces mature guard cells (Lai *et al.*, 2005; Raissig *et al.*, 2017). Stomatal spacing is partly regulated via signaling peptides from the EPF family. Upon initiation of stomatal fate, the SPCH:ICE complex stimulates the production of EPFs in the guard mother cell. In *Arabidopsis*, these EPF peptides radiate from the guard mother cell and compete with the positive regulator STOMAGEN (Sugano *et al.*, 2010) to bind ERECTA/ERECTA-LIKE (ER/ERL) receptors in a concentration-dependent manner (Torii, 2021). The binding triggers a mitogen-activated protein kinase signaling cascade that passes through the EMBRYO DEFECTIVE 71 (YDA) gene to phosphorylate SPCH (Bergmann *et al.*, 2004). Phosphorylation of SPCH inhibits SPCH:ICE heterodimerization that prevents stomatal fate in the surrounding pavement cells (Abrash *et al.*, 2018).

Expressing or overexpressing EPF family members has resulted in reduced SD in many C_3 species, suggesting that function is largely conserved across C_3 monocots and dicots (Hepworth *et al.*, 2015; Wang *et al.*, 2016; Hughes *et al.*, 2017; Caine *et al.*, 2019; Dunn *et al.*, 2019; Mohammed *et al.*, 2019; Jiao *et al.*, 2022; Karavolias *et al.*, 2023). However, the possibility of neofunctionalization or functional redundancy among EPFs in C_4 species has received less attention despite evidence that the evolution of Kranz anatomy is associated with changes in the role of SHR and SCARECROW in leaf development (Schuler *et al.*, 2018; Hughes *et al.*, 2023). In sorghum, overexpression of EPF1 had very mild effects on SD relative to rice (Caine *et al.*, 2019), wheat (Dunn *et al.*, 2019), or barley (Hughes *et al.*, 2017), while expression of a synthetic EPF2 reduced SD and increased iWUE similar to other species (Franks *et al.*, 2015; Ferguson *et al.*, 2024). Therefore, the apparent functional conservation of EPF genes means that they are excellent candidates for producing model systems to study the effects of reduced SD in C_4 species.

Our study was motivated by the need to understand better the relationship between SD and g_{sw} in crop species. Sugarcane was explored as a case study system for C_4 species. Sugarcane

is the leading crop in biomass production and provides 80% of the global table sugar and 40% of the world's biofuel (Budeguer *et al.*, 2021). We aimed to (i) modulate an EPF gene to engineer sugarcane with lower SD and g_{sw} ; (ii) quantify changes in epidermal cell patterning and stomatal complex size; (iii) estimate the consequences of altered stomatal patterning for maximum potential g_{sw} ; (iv) assess changes in g_{sw} and photosynthetic physiology arising from altered SD; and (v) perform a meta-analysis to summarize the quantitative relationship between lower SD and reduced g_{sw} across C_3 and C_4 species from dicot and monocot lineages.

Materials and methods

Construct design and generation

A BLAST search of the *Sorghum bicolor* genome using *Arabidopsis thaliana* (*Arabidopsis*) EPF2 (At1G34254) identified Sobic.006G104400 with 69% sequence identity that we named SbEPF2. We amplified this sequence from sorghum before cloning the amplicon into plasmid pPTN1434 to create expression cassettes containing SbEPF2 and neomycin phosphotransferase II (*nptII*). The 5'-untranslated region (UTR), EPF2 coding sequence, and 3'-UTR from *S. bicolor* were used for this vector construct. SbEPF2 was placed under transcriptional control of the ubiquitin promoter from *Zea mays* with its first intron (ZmUbi) and the 35S poly(A) signal from cauliflower mosaic virus (CaMV). The selectable marker gene *nptII* was under transcriptional control of the 35S promoter and the 35S poly(A) signal from the CaMV.

Generation of transgenic sugarcane

Plasmid pPTN1434, containing SbEPF2 and *nptII* expression cassettes, was introduced into sugarcane callus CP88-1762 by biolistic gene transfer as described by Taparua *et al.* (2012). Briefly, leaf whorl cross-sections of CP88-1762 were cultured on modified Murashige and Skoog medium (MS) with B5 vitamins (PhytoTech Labs, KS, USA) supplemented with 3 mg Γ^{-1} 2,4-dichlorophenoxyacetic acid (PhytoTech Labs, KS, USA) to initiate embryogenic calli. Leaf whorl cultures were maintained at 28 °C in an incubator in the dark and subcultured every 14 d. Eight weeks after culture initiation, linearized expression cassettes were precipitated onto 1 μ m gold particles and introduced into embryogenic calli using a biolistic PDS-1000/He delivery system (Bio-Rad, Hercules, CA, USA). One week after gene transfer, calli were transferred to a medium containing 20 mg Γ^{-1} geneticin (PhytoTech Labs) to select transgenic events. Following 5 weeks of antibiotic selection, calli were subcultured onto regeneration medium [MS medium with B5 vitamins, supplemented with 1.86 mg Γ^{-1} α -naphthaleneacetic acid (NAA; PhytoTech Labs) and 0.09 mg Γ^{-1} 6-benzylaminopurine (BAP; PhytoTech Labs), and were maintained at 28 °C in an incubator with a 16/8 h light (100 μ mol $m^{-2} s^{-1}$) and dark cycle. Regenerated shoots >1 cm in length were transferred to a modified MS basal medium with 4.4 g Γ^{-1} Gamborg vitamins (PhytoTech Labs) for shoot elongation and rooting. Rooted plantlets were transferred to soil and acclimatized in a temperature-controlled plant growth chamber maintained at 28 °C day and 22 °C night temperature with a 16/8 h light (400 μ mol $m^{-2} s^{-1}$) and dark cycle for further analysis.

Analysis of transgene expression by quantitative reverse transcription-PCR

Transcript levels of SbEPF2 in the wild type and transgenics were determined by quantitative reverse transcription-PCR (RT-qPCR) analysis. We sampled the differentiation zone above the ligule from the wild

type, plus events 15 and 38. We extracted RNA from these samples using the Monarch Total RNA Extraction and Purification kit (New England Biolabs). The RNA was normalized between samples to 100 ng μl^{-1} before conducting the RT-qPCR using the Luna One-Step RT-qPCR kit (New England Biolabs) on a BioRad CFX Connect Real-Time System (BioRad). Transcript levels of SbEPF2 were normalized against the glyceraldehyde-3-phosphate dehydrogenase (ShGAPDH) gene. Primers used were ShGAPDH_forward (CACGGCCACTGGAAGC), ShGAPDH_reverse (TCCTCAGGGTTCCTGATGCC), SbEPF2_forward (CGACGAGCTAGCAGGAAGAG), and SbEPF2_reverse (GGGGATCCTGTGATGTGAGC).

Experimental design and environmental conditions for phenotyping assays

The experimental materials were vegetatively propagated, transgenic events from sugarcane cultivar CP 88-1762. Following regeneration of putative transgenic plants, PCR was used as the initial screen to confirm transgene presence in genomic DNA extracts. One plant from each of the 18 independent events was screened for reduced SD before selecting the two with the highest decrease (SbEPF2-15 and SbEPF2-38) for further propagation and testing. Ten vegetatively propagated replicates of each transgenic event plus the wild type were grown in a randomized block design for detailed phenotyping. Stomatal density, leaf photosynthetic gas exchange, specific leaf area (SLA), leaf N content, and chlorophyll content were assessed on all plants. Additional detailed evaluation of epidermal patterning and anatomical determinants of maximum g_s ($g_{s\max}$) were assessed on SbEPF2-15. All plants were grown under greenhouse conditions where a 15 h photoperiod was provided by combining natural irradiance with supplemental LEDs with a minimum light intensity threshold of 1500 $\mu\text{mol m}^{-2} \text{s}^{-1}$. Air temperature was controlled between 27 °C and 30 °C, and 21 °C and 23 °C during day and night periods, respectively.

Measuring stomatal density and spatial patterning

An optical tomographer was used to rapidly image the leaf epidermis using established protocols (Xie *et al.*, 2021). Each genotype was sampled by cutting a small section from a central position on the youngest fully expanded leaf. Samples were placed on dry ice and imaged within 30 min. A MarSurf CM Explorer (Mahr) scanned the leaf sample at $\times 20$ magnification to produce images with a size of 800 \times 800 μm^2 . The upper and lower z -scale limits were set manually to capture all stomata in four fields of view interspersed along a transect from the midrib to the margin of each leaf surface. The images were measured for traits relating to stomata density, stomatal epidermal patterning, bulliform epidermal patterning, prickle epidermal patterning, and stomatal complex dimensions. Average values from the four fields of view formed the technical replicate of each biological replicate. Cell counts, cell sizes, and spatial measurements were taken with ImageJ Fiji using the schema shown in the appropriate figures. Calculations of maximum aperture size and maximum theoretical stomatal conductance ($g_{s\max}$) were made as detailed in Al-Salman *et al.* (2023). Maximum pore aperture (a_{\max}) was calculated in μm^2 by multiplying stomatal complex width (Sto_{width}) with length (Sto_{length}).

$$a_{\max} = Sto_{\text{width}} \times Sto_{\text{length}}$$

$g_{s\max}$ was calculated in $\text{mol m}^{-2} \text{s}^{-1}$. Here d =diffusivity of water vapor in air; v =molar air volume of 24.8 $\text{mol}^{-1} \text{dm}^3$ under reference atmospheric pressure and greenhouse temperature of 30 °C; I =stomatal pore depth assumed to be $Sto_{\text{width}}/2$; SD=stomatal density; and a_{\max} =maximum pore aperture.

$$g_{s\max} = \frac{d}{v} \left(\frac{SD \times a_{\max}}{I + \frac{\pi}{2} \sqrt{\frac{a_{\max}}{\pi}}} \right)$$

Gas exchange measurements

Steady-state, light-saturated gas exchange measurements were taken using the LI-COR 6800 gas analyzer (LI-COR Biosciences, Lincoln, NE, USA). All measurements were made in the center of the youngest fully expanded leaf. Chamber conditions were maintained at a photosynthetic photon flux density (PPFD) of 2000 $\mu\text{mol m}^{-2} \text{s}^{-1}$ (10% blue and 90% red light), chamber $[\text{CO}_2]$ of 450 ppm, temperature of 30 °C, and 60–70% relative humidity to assess leaf gas exchange at growth $[\text{CO}_2]$. Additional data were collected after making step-changes in $[\text{CO}_2]$ from 450 to 250, 50, and 20 ppm once equilibrium was reached in the chamber to assess leaf gas exchange under conditions that promote stomatal opening.

Leaf chlorophyll, nitrogen content, and specific leaf area

Relative chlorophyll content was estimated using a handheld SPAD-502 Plus chlorophyll meter (Konica Minolta, Tokyo, Japan). Leaf N content and SLA were assessed following the protocols of Markelz *et al.* (2011). Leaves were sampled in the greenhouse using a hole punch with an area of 4 cm^2 . These leaf discs were transferred to a drying oven set at 60 °C for 2 weeks. The dry mass of each sample was determined before being combusted in an elemental analyzer (Elemental Combustion System, Costech). The SLA was calculated as the ratio of leaf area to dry leaf mass ($\text{cm}^2 \text{g}^{-1}$).

Meta-analysis

The literature was screened for experiments where g_{sw} was measured in transgenic plants with low SD as a result of perturbing expression of genes activating the SPCH/ICE basic helix–loop–helix (bHLH) stomatal development pathway. The search terms used in our searches were ‘stomatal density’ or ‘stomatal conductance’ with ‘WUE’. Each hit in the literature search was used to mine other studies using their reference section. This approach produced a dataset for 10 species from three functional groups, comprising *A. thaliana* (C_3 dicot), *Hordeum vulgare* (barley, C_3 monocot), *Oryza sativa* (rice, C_3 monocot), *Populus tremuloides* (poplar, C_3 dicot), *Saccharum* spp. (sugarcane, C_4 monocot), *Solanum lycopersicum* (tomato, C_3 dicot), *Sorghum bicolor* (sorghum, C_4 monocot), *Triticum aestivum* (wheat, C_3 monocot), *Vitis vinifera* (grape, C_3 dicot), and *Zea mays* (maize, C_4 monocot), along with the data reported in the current study (data sources: Dow *et al.*, 2014; Hepworth *et al.*, 2015; Liu *et al.*, 2015; Shen *et al.*, 2015; Wang *et al.*, 2016; Hughes *et al.*, 2017; Caine *et al.*, 2019; Dunn *et al.*, 2019; Mohammed *et al.*, 2019; Li *et al.*, 2021; Clemens *et al.*, 2022; Jiao *et al.*, 2022; Karavolias *et al.*, 2023). Data were gathered from multiple transgenic events in a single study if SD and g_{sw} were reported for each line. Studies in the meta-analysis did not discriminate between plants in growth chambers and greenhouse conditions. We calculated the percentage changes in SD and g_{sw} relative to the wild type to normalize the data between studies. The data were limited to measurements of g_s collected on leaves experiencing a CO_2 range between 400 ppm and 500 ppm to simulate ambient atmospheric conditions.

Statistical analysis and modeling

Plants were independent replicates of each genotype with $n=10$. The initial screen was analyzed using a two-way ANOVA, with all subsequent analyses conducted using a linear mixed-effects model with post-hoc

pairwise comparisons. The model fitted a fixed dependent and independent variable, with the random effect being block number using the Python library Pymer4 (Jolly, 2018). Meta-analysis was conducted by linear regression using a least-squares method with the `linegress` function in the Python library SciPy.

Results

We hypothesized that overexpressing an EPF2 ortholog in sugarcane would increase the negative regulation of stomatal development and reduce SD. On average, across 18 SbEPF2-expressing transgenic events in an initial screen, SD was 17% lower than in the wild type on the abaxial leaf surface (Supplementary Fig. S1). We selected two lines (SbEPF2-15 and SbEPF2-38) where the reduction in SD compared with the wild type was stronger than average. After vegetatively propagating lines SbEPF2-15 and SbEPF2-38 to the following generation, we sampled the stomatal development zone in leaves to confirm the presence of SbEPF2 by RT-qPCR. Transcriptional analysis showed that both transgenic lines had significant SbEPF2 expression in the leaf stomatal development zone, but no signal was detected in wild-type plants (Supplementary Fig. S2). The more replicated assessment of SD showed that each transgenic line displayed a stronger reduction in SD. Adaxial SD was 38% and 35% lower than in the wild type in SbEPF2-15 and SbEPF2-38, respectively (Fig. 1A). Abaxial responses were weaker, with SD being 26% lower than that of the wild type in both transgenic lines (Fig. 1B).

Sugarcane epidermal cells are arranged in straight files that run in a longitudinal direction along the leaf (Fig. 2). Additional detailed evaluation of epidermal patterning in SbEPF2-15 showed that the reduction in SD on both leaf surfaces compared with the wild type was driven by a reduction in the: (i) density of cell files containing stomata (adaxial -21%, abaxial -9%, Fig. 2A, D) and (ii) density of stomata within cell files (adaxial -24%, abaxial -19%; Fig. 2C, F); that is, greater spacing between stomata. The greater spacing between stomatal cell files was itself partly due to 'stomatal regions' (i.e. zones of intercostal cells, not including bulliform cells) being wider (adaxial +17%, abaxial +17%) in SbEPF2-15 than the wild type (Fig. 2B). Almost all stomatal regions on the adaxial surface contained only a single file of stomata surrounded by intercostal pavement cells and this did not differ between SbEPF2-15 and the wild type (Supplementary Fig. S3A). By contrast, 44% of stomatal regions on the abaxial surface contained multiple files of stomata (Supplementary Fig. S3B). The increased number of stomatal regions with multiple stomata-containing files contributed to the greater SD on the abaxial versus adaxial surface but did not differ between SbEPF2-15 and the wild type.

We measured the same traits in prickle and bulliform cells to study the impact of reduced SD on other major epidermal cell types. SbEPF2-15 was not significantly different from the wild type in the density of bulliform cells, the density of bulliform

cell files, the width of bulliform regions, or the frequency of bulliform cells within a file (Supplementary Fig. S4). By contrast, the prickle density of SbEPF2-15 was lower than that of the wild type by 35% on the adaxial surface and 14% on the abaxial surface (Fig. 3A, E). Unlike stomata, the reduction in prickle density was not associated with a significant change in the density of cell files containing prickles (Fig. 3B, F) and was dominated by a reduction in the density of prickles within a cell file (adaxial -25%, abaxial 8%; Fig. 3D, H). Correspondingly, there was no difference between SbEPF2-15 and the wild type in the width of prickle regions (i.e. costal zones; Fig. 3C, G; Supplementary Fig. S5).

We measured stomatal complex size and then calculated maximum aperture size and g_{smax} to determine if reduced SD altered these traits. Reduced SD in SbEPF2-15 compared with the wild type was not accompanied by significant changes in stomatal complex length or width on either leaf surface (Fig. 4A, B, E, F). Consequently, there was no significant difference between SbEPF2-15 and the wild type in the modeled maximum stomatal aperture on either leaf surface (Fig. 4C, G). However, the reductions in SD led to significantly lower g_{smax} in SbEPF2-15 compared with the wild type (-24% adaxial, -30% abaxial; Fig. 4D, H).

We measured gas exchange and proxies for photosynthetic capacity in the two low-SD transgenic lines. There were no significant differences between either transgenic or wild type in A_n (Fig. 5A), g_{sw} (Fig. 5B), or iWUE (Fig. 5C). There were also no significant differences between the wild type and either transgenic line in SLA (Fig. 5D), relative chlorophyll content (Fig. 5E), or leaf N concentration (Fig. 5F). We then re-measured g_{sw} at a range of $[CO_2]$ to explore how stomatal aperture may be modulating the effects of SD on leaf gas exchange (Fig. 6). Consistent with our previous results, there was no difference in g_{sw} between either transgenic line and the wild type at 450 ppm. However, as $[CO_2]$ was progressively reduced, the transgenic lines did not increase g_{sw} in the same manner as the wild type. Consequently, when stomata were open close to their maximum extent at 20 ppm CO_2 , g_{sw} of the transgenic lines was reduced relative to the wild type by 24–28% (Fig. 6).

The gas exchange measurements made us question the relationship between SD and g_{sw} in plants engineered to have reduced SD. Meta-analysis of previously published data revealed a significant correlation between engineered reductions in SD and reductions in g_{sw} (Fig. 7), with the relationship being strong for C_4 monocots ($P=0.001$, $r^2=0.97$) and C_3 monocots ($P=0.001$, $r^2=0.87$), but modest for C_3 dicots ($P=0.032$, $r^2=0.59$). In most cases, the reduction in g_{sw} was smaller than the reduction in SD. It was especially clear in monocots, where the reduction in g_{sw} only matched the magnitude of the reduction in SD in one case, and the intercept of the regression lines indicated that no change in g_{sw} would be expected given a 7–25% change in SD for C_3 and C_4 species, respectively.

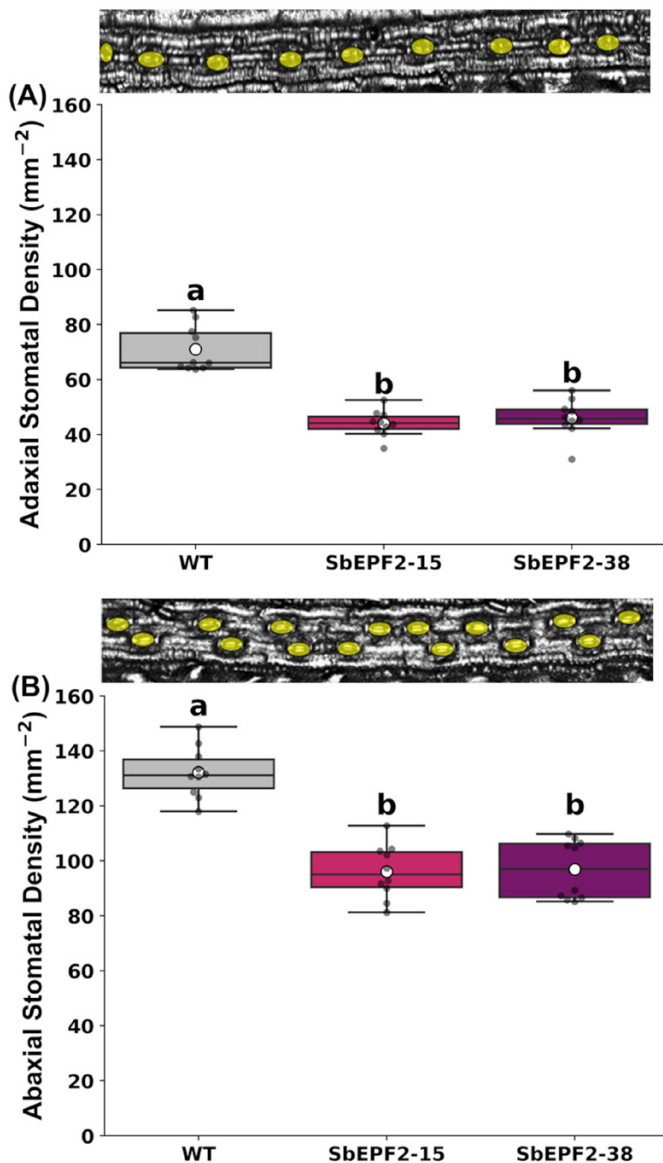


Fig. 1. Stomatal density of wild-type (WT) transgenic sugarcane overexpressing SbEPF2 (SbEPF2-15 and SbEPF2-38). (A) Adaxial and (B) abaxial stomatal density (mm^{-2}), with images above providing an example of WT stomatal patterning. Graphs show box plots of the 25th and 75th percentile, with a line indicating the median value. Each box plot shows the mean with a white circle, and gray dots showing individual observed residual data points ($n=10$), where letters within each panel indicate significant differences between genotypes.

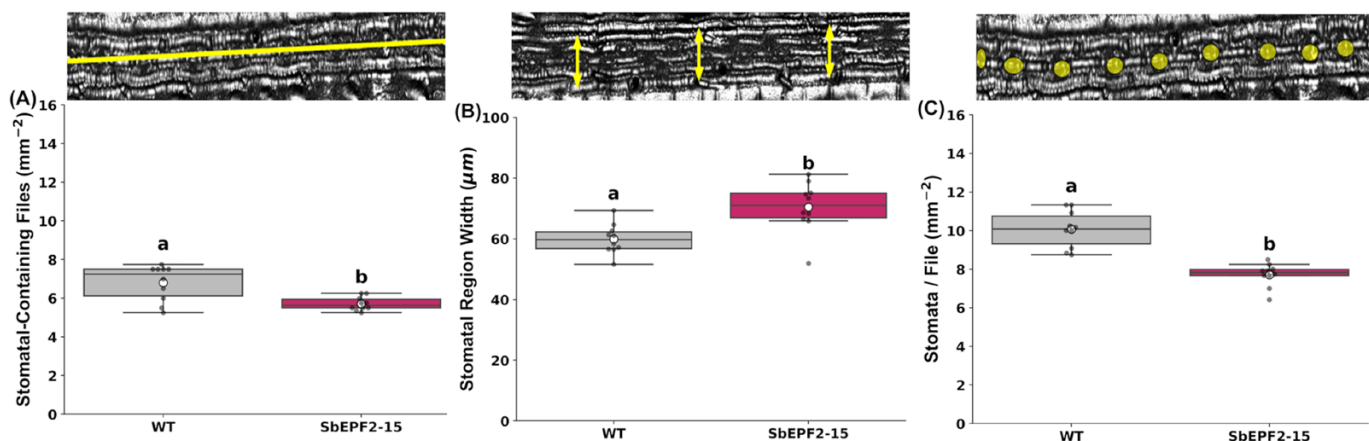
Discussion

This study advanced understanding of how altering the expression of stomatal development genes influences epidermal anatomy and leaf photosynthetic gas exchange by successfully addressing five aims. First, sugarcane, a species representing understudied but agriculturally important polyploid C_4 grass crops, was engineered to have reduced SD. Second, reductions in SD were found to result in roughly equal reductions in the

density of cell files containing stomata and decreases of stomata within a cell file. The altered epidermal pattern was accompanied by reductions in the density of prickly cells but not bulliform cells. Reducing SD did not alter the stomatal complex size. Third, reducing SD by 38% on the adaxial surface and 26% on the abaxial surface was predicted to reduce g_{smax} by 24% on the adaxial surface and 30% on the abaxial surface from our meta-analysis (Fig. 7). Fourth, there was no commensurate change in operating g_{sw} when it was assessed by measurement of leaf gas exchange, along with no change in A_n or proxies for photosynthetic capacity (leaf N, SLA, and chlorophyll content). This outcome appears to have been driven by increased stomatal aperture that completely compensated for the reduction in SD. Fifth, meta-analysis revealed that ameliorating the effects of reduced SD on g_{sw} by increasing stomatal complex size and/or stomatal aperture is likely to be a general phenomenon across C_3 and C_4 species from both monocot and dicot lineages. The sugarcane engineered in this study would represent the most extreme case reported to date of stomatal behavior ameliorating the effects of stomatal anatomy on g_{sw} . It has the potential to provide a powerful experimental system for future studies on the mechanisms underlying a phenomenon with important implications for efforts to improve crop WUE.

Reducing stomatal conductance by lowering SD has proven successful in engineering crops with increased iWUE (Dow *et al.*, 2014; Hepworth *et al.*, 2015; Liu *et al.*, 2015; Shen *et al.*, 2015; Wang *et al.*, 2016; Caine *et al.*, 2019; Dunn *et al.*, 2019; Mohammed *et al.*, 2019; Li *et al.*, 2021; Clemens *et al.*, 2022; Jiao *et al.*, 2022; Karavolias *et al.*, 2023). However, C_4 species have been understudied in this regard despite the potential for beneficial outcomes (Leakey *et al.* 2019). In addition, the quantitative relationship between engineered changes in SD and g_{sw} has not been summarized despite evidence for compensatory changes in stomatal complex size and stomatal aperture. To further explore this relationship in a C_4 species, we reduced SD in sugarcane by expressing a sorghum EPF. We identified a potential EPF ortholog *Sobic.006G104400* in sorghum (SbEPF2) that was 69% identical to *Arabidopsis AtEPF2* (Hunt and Gray, 2009). When expressed in sugarcane, SbEPF2 decreased adaxial and abaxial SD by 35–38% and 26%, respectively (Fig. 2). These *in silico* and phenotypic data show SbEPF2 encodes a functional EPF ortholog. Qualitatively, functional conservation of SbEPF2 in sugarcane was expected, given that other experiments reported reduced SD when overexpressing EPFs in various species (Hughes *et al.*, 2017; Caine *et al.*, 2019; Dunn *et al.*, 2019; Mohammed *et al.*, 2019; Karavolias *et al.*, 2023). However, the reduction in SD was lower in our transgenics than those observed when a native EPF was overexpressed in grass species. Interestingly, transgenically expressing EPFs from various grass species in *Arabidopsis* produced a far lower reduction of SD than when overexpressed in the native species in several other reports (Hughes *et al.*, 2017; Caine *et al.*, 2019; Dunn *et al.*, 2019). The relatively low SD reduction observed in this report and other expression experiments may be due to sorghum

Adaxial



Abaxial

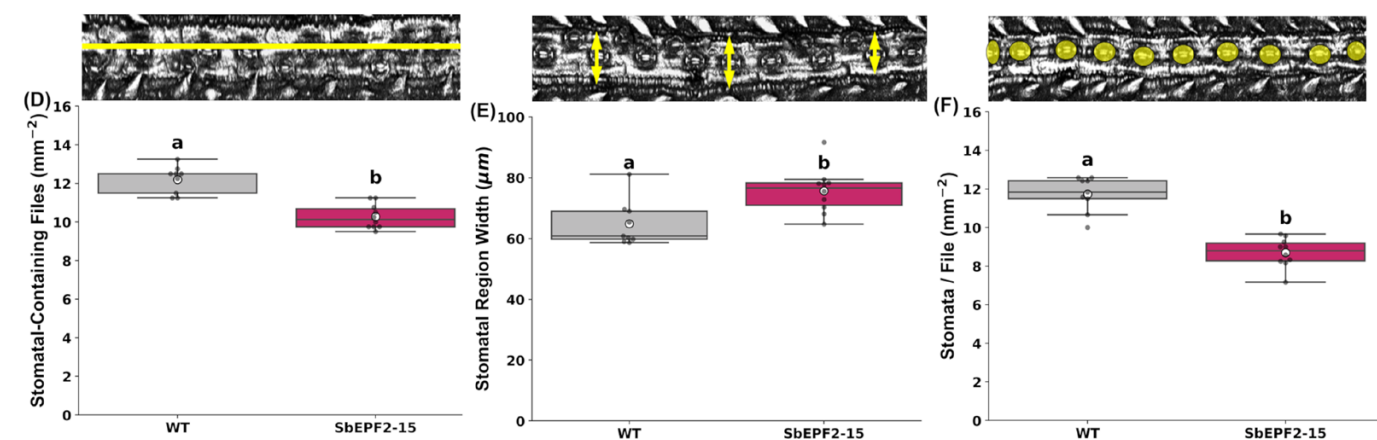


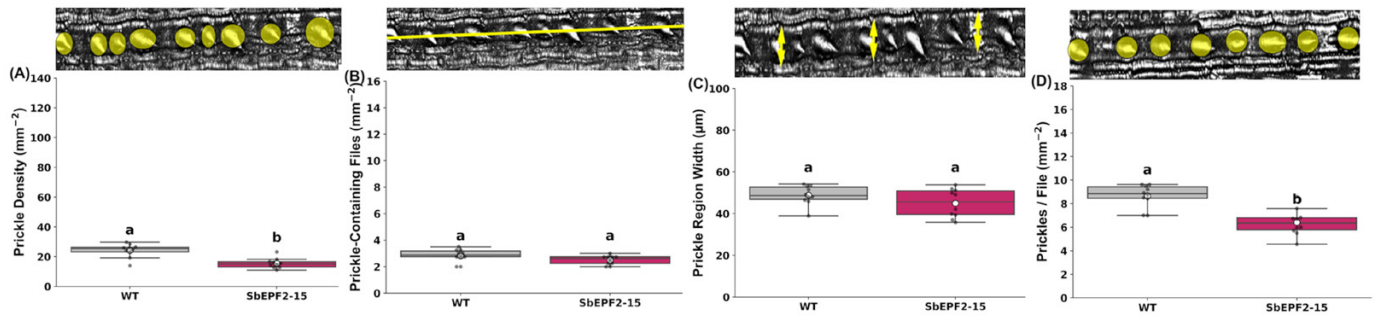
Fig. 2. Stomatal epidermal patterning of wild-type (WT) transgenic sugarcane overexpressing *SbEPF2* (*SbEPF2-15*). (A) Adaxial stomata-containing files; (B) adaxial stomatal region width (μm); (C) adaxial stomata per file; (D) abaxial stomata-containing files; (E) abaxial stomatal region width (μm); and (F) abaxial stomata per file with WT images above showing how each trait was measured. Graphs show box plots of the 25th and 75th percentile, with a line indicating the median value. Each box plot shows the mean with a white circle, and gray dots showing individual observed residual data points ($n=10$), where letters within each panel indicate significant differences between genotypes.

and sugarcane *EPF2* orthologs not having complete functional conservation. Sugarcane expressing *SbEPF2* may inefficiently bind ER/ERL receptors, limiting the strength of negative repression relative to native *EPF* orthologs. How efficiently non-native *EPF* genes bind ER/ERL compared with the native *EPF* peptides is unknown and deserves future exploration.

Previous experiments that utilize *EPFs* in grasses to lower SD reported that this was driven by reducing the stomatal index (i.e., ratio of stomata to number of epidermal cells) as a result of stomatal development arresting at several different stages (Hughes *et al.*, 2017; Caine *et al.*, 2019; Dunn *et al.*, 2019). In grasses, variation in SD can also be characterized by changes in the number of cell files containing stomata and the density of stomata within a cell file. In sugarcane, both of these mechanisms contributed to the reduction in SD resulting from *SbEPF2* expression. However, the reduction of stomata within a file was greater (adaxial -24% , abaxial -19% ; Fig. 2C, F) than

the reduction in the density of files containing stomata (adaxial -21% , abaxial -9% ; Fig. 2A, D) on both leaf surfaces. Additional analyses will be needed to fully understand if the reduced density of cell files containing stomata results from changes in cell identity or cell expansion. Cell expansion seems the most likely candidate mechanism since *SHORTROOT* acts to regulate the formation of cell files containing stomata (Schuler *et al.*, 2018; Wu *et al.*, 2019), and this occurs upstream of the stomatal development pathway (Zoulias *et al.*, 2018). This notion is also supported by the greater width of intercostal regions that contain stomata without changing the number of stomata-containing files within each region in the *SbEPF2* plants (Fig. 2A, B, D, E; Supplementary Fig. S3). Meanwhile, the reduced density of stomata within cell files is consistent with the expression of the *SbEPF2* triggering the signaling cascade by which the *EPF* family is well known to determine stomatal fate in various species (Zoulias *et al.*, 2018).

Adaxial



Abaxial

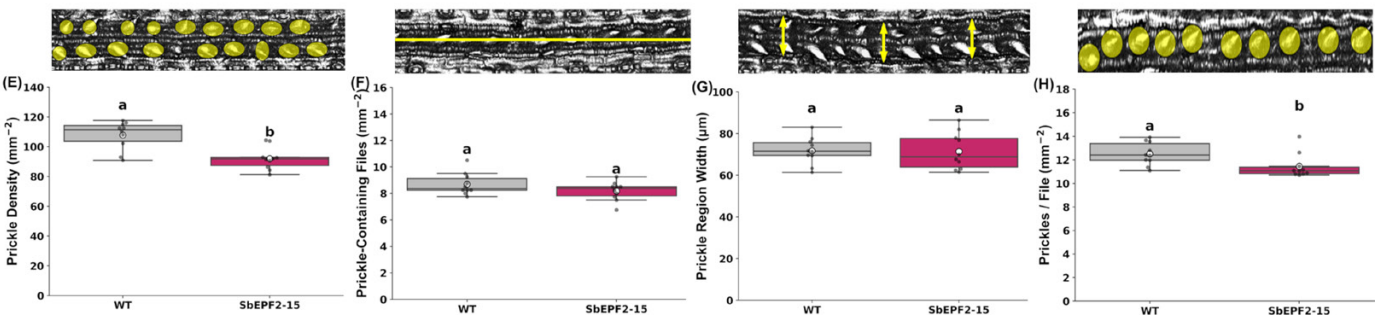


Fig. 3. Prickle epidermal patterning of wild-type (WT) transgenic sugarcane overexpressing SbEPF2 (SbEPF2-15). (A) Adaxial prickle density (mm^{-2}); (B) adaxial prickle-containing files; (C) adaxial prickle region width (μm); (D) adaxial prickles per file; (E) abaxial prickle density (mm^{-2}); (F) abaxial prickle-containing files; (G) abaxial prickle region width (μm); and (H) abaxial prickles per file, with WT images above showing how each trait was measured. Graphs show box plots of the 25th and 75th percentile, with a line indicating the median value. Each box plot shows the mean with a white circle, and gray dots showing individual observed residual data points ($n=10$), where letters within each panel indicate significant differences between genotypes.

There is evidence for the interplay of stomatal development with hair cells and other specialized epidermal cells (Torii, 2021; Nunes *et al.*, 2023). However, this broad topic, including specifically whether EPF family members play a role in influencing prickle and bulliform development in grasses, is underexplored. Ubiquitous expression of SbEPF2 in sugarcane did not alter bulliform cell density and patterning (Supplementary Fig. S4), the density of prickle-containing files, or the width of costal regions containing prickles (Fig. 3C, G). Previous studies have reported negative correlations between the number of stomata and the number of hairs or trichomes in *Brachypodium* (Raissig *et al.*, 2016; Abrash *et al.*, 2018), maize (Kong *et al.*, 2021), and tomato (Galdon-Armero *et al.*, 2018). These data suggest that the two classes of cells share common pathways early in their development before a subsequent divergence. Prickle cell density and the density of prickles along a cell file decreased in SbEPF2 plants on both leaf surfaces (Fig. 3). This shared response of stomata and prickles to SbEPF2 expression is consistent with evidence from a YODA mutant in *Brachypodium* with greater stomatal and hair cell density implying that common pathways can be involved in regulating spacing between the two cell types (Abrash *et al.*, 2018). In addition, a hair cell-specific peroxidase regulates the size of both hair cells and stomata in *Brachypodium*, with consequences for g_{sw} (Nunes *et al.*, 2023). These studies shed further light on how epidermal patterning

is regulated and how changes in the density and size of hairs may alter leaf boundary layer conductance (Schreuder *et al.*, 2001; Roth-Nebelsick *et al.*, 2009) and interact with stomatal anatomy to determine leaf gas exchange fluxes.

Model predictions of g_{smax} from anatomical measurements of SD and stomatal complex size for plants expressing SbEPF2 were 25% lower on the adaxial surface and 30% lower on the abaxial surface when compared with the wild type (Fig. 6D, H). This model reinforces the expectation that plants expressing SbEPF2 would have reduced g_{sw} , as observed in previous studies where EPF expression was modified to reduce SD (Dow *et al.*, 2014; Hepworth *et al.*, 2015; Liu *et al.*, 2015; Shen *et al.*, 2015; Wang *et al.*, 2016; Hughes *et al.*, 2017; Caine *et al.*, 2019; Dunn *et al.*, 2019; Mohammed *et al.*, 2019; Li *et al.*, 2021; Clemens *et al.*, 2022; Jiao *et al.*, 2022; Karavolias *et al.*, 2023). However, both transgenic lines expressing SbEPF2 showed no change in g_{sw} compared with the wild-type control (Fig. 5B). This was surprising because meaningful reductions in g_{sw} have been observed in other species when SD was reduced to a similar degree to that in sugarcane (Fig. 7), but not unprecedented because one event of an *epfl10* knockout in rice had 20% lower SD but showed no change in g_{sw} with similar-sized stomatal complexes and increased pore aperture (Karavolias *et al.*, 2023).

In several previous studies, reductions in SD have been accompanied by increases in stomatal complex size and/or

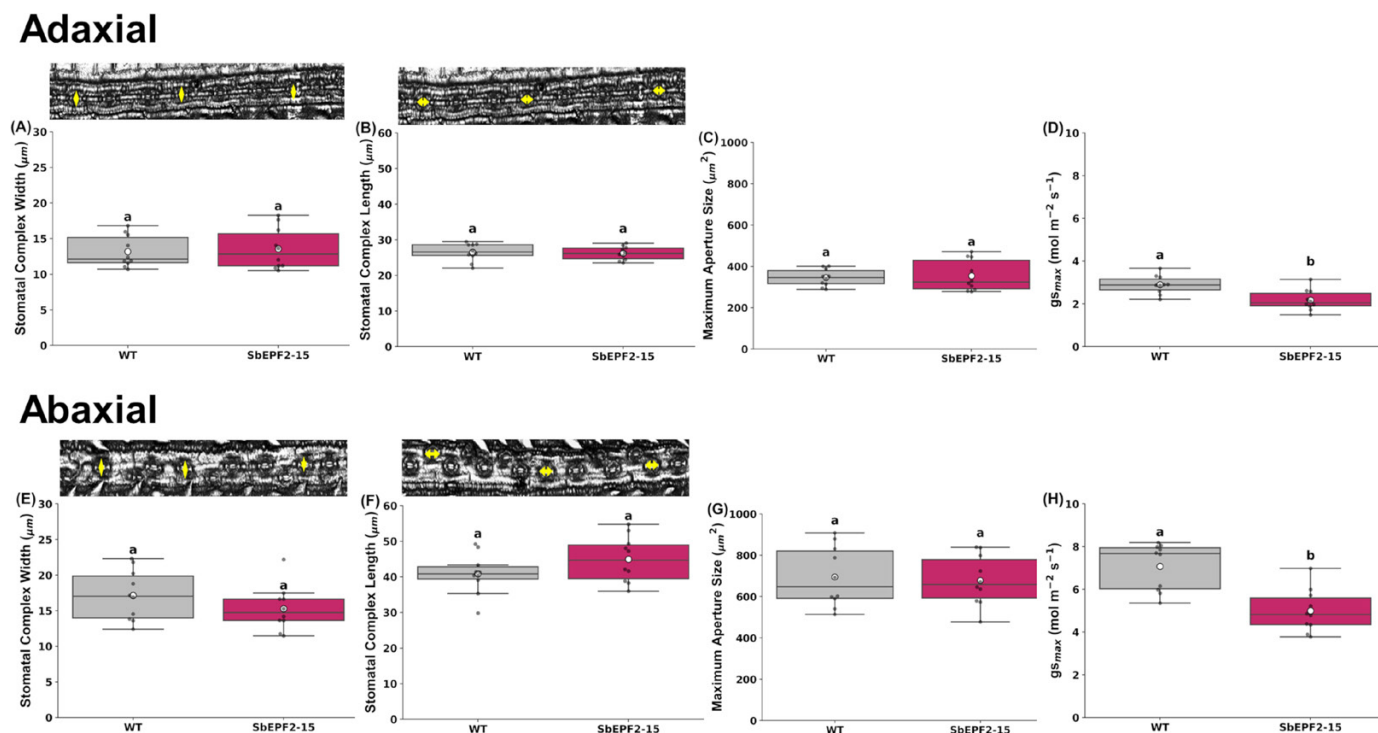


Fig. 4. Stomatal complex measurements of wild-type (WT) transgenic sugarcane overexpressing SbEPF2 (SbEPF2-15). (A) Adaxial stomatal complex width (μm); (B) adaxial stomatal complex length (μm); (C) adaxial A_{max} (μm^2); (D) adaxial $g_{\text{sw,max}}$; (E) abaxial stomatal complex width (μm); (F) abaxial stomatal complex length (μm); (G) abaxial A_{max} (μm^2); and (H) abaxial $g_{\text{sw,max}}$, with WT images above showing how each trait was measured. Graphs show box plots of the 25th and 75th percentile, with a line indicating the median value. Each box plot shows the mean with a white circle, and gray dots showing individual observed residual data points ($n=10$), where letters within each panel indicate significant differences between genotypes.

stomatal aperture that were thought to ameliorate the reduction in g_{sw} (Büßis *et al.*, 2006; Franks *et al.*, 2015; Zhu *et al.*, 2015; Wang *et al.*, 2016; Caine *et al.*, 2019; Mohammed *et al.*, 2019; Zhao *et al.*, 2020; Li *et al.*, 2021; Karavolias *et al.*, 2023). However, other studies have reported no such compensating changes in stomatal anatomy, stomatal physiology, or reductions in stomatal complex size that would tend to increase reductions in g_{sw} (Hughes *et al.* 2017; Caine *et al.* 2019). Notably, greater stomatal apertures could result from two different but not mutually exclusive mechanisms. First, if larger stomatal complexes develop on low-SD plants and open to the same fraction of their maximum aperture, their aperture would be greater than that of the wild type. Second, guard cells act to open stomata to a larger fraction of their maximum aperture than the wild type without any change in stomatal complex size. The mechanisms underpinning these two responses in plants engineered to have lower SD are unknown. Addressing this knowledge gap is potentially challenging because the contribution of the two mechanisms seems to vary between species and even genotypes or experiments. This variation in g_{sw} is the result of complex interactions between SD, stomatal complex size, and stomatal opening (Franks *et al.*, 2009), all of which are dynamically influenced by environmental conditions and A_n (Long and Bernacchi, 2003; Wolz *et al.*, 2017).

The sugarcane expressing SbEPF2 developed in this present study is a potentially valuable system to study further how stomatal behavior changes in plants engineered to have low SD. First, the absence of any change in g_{sw} despite 38% and 26% reductions in SD on the adaxial and abaxial surfaces, respectively, means that there would be no change in transpiration and no feedback effects on water relations that would result from changes in the rate of plant water use. Second, in a C_4 system under contemporary atmospheric $[\text{CO}_2]$, if modest reductions in g_{sw} did occur, they would not increase stomatal limitation to A_n , and feedback effects from altered carbon gain would not occur (Leakey *et al.*, 2019). Third, SbEPF2-expressing plants did not differ from the wild type in proxies for photosynthetic capacity (Fig. 5), which can influence g_{sw} in other systems (Franks *et al.*, 2015; Ferguson *et al.*, 2024). Under these circumstances, there was no change in the size of the stomatal complex in sugarcane expressing SbEPF2 (Fig. 4). The most parsimonious explanation for no response in operating g_{sw} to the reduction in SD is an increase in stomatal aperture. Stomatal aperture has been estimated either by pressing imprint material onto leaf surfaces in a way that captures a mold of the stomatal pore that can be measured under a microscope (Büßis *et al.*, 2006) or by using a razor blade to dissect away leaf tissue, leaving an epidermal peel where the pore aperture can

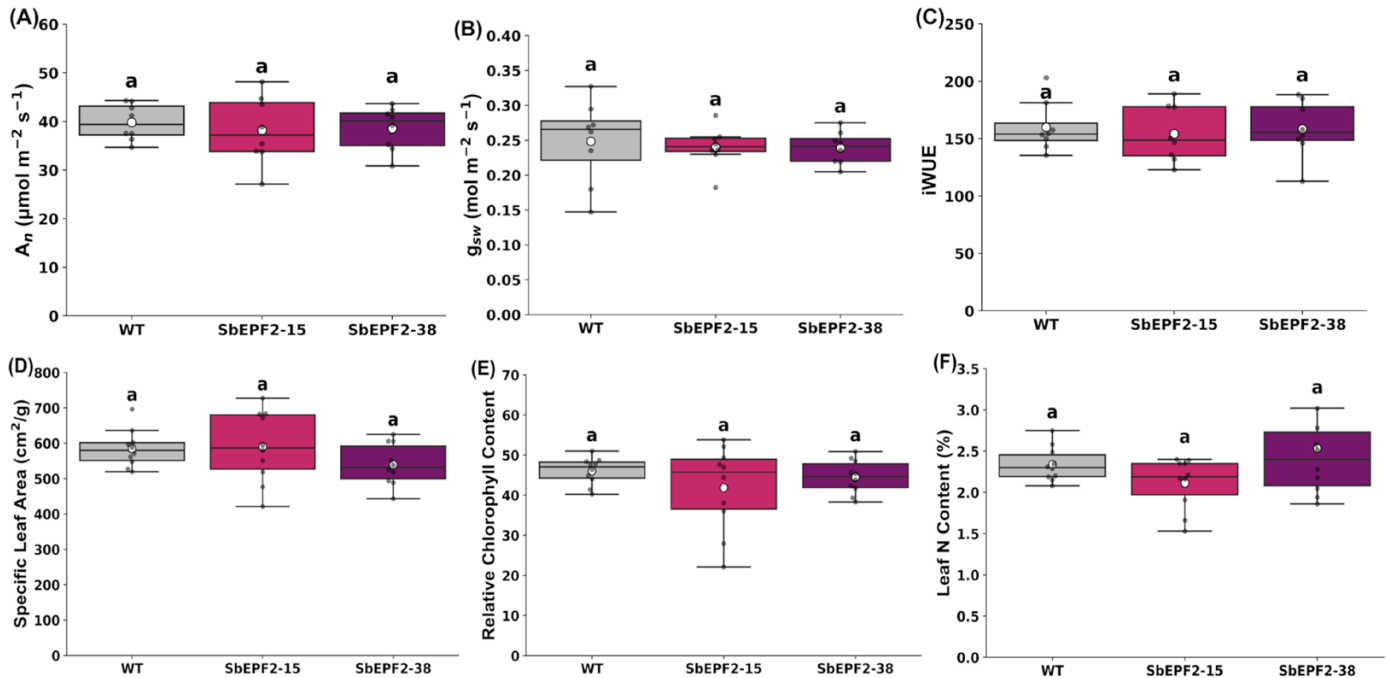


Fig. 5. Leaf physiology of wild-type (WT) transgenic sugarcane overexpressing SbEPF2 (SbEPF2-15 and SbEPF2-38). (A) Carbon assimilation (A_n); (B) stomatal conductance (g_{sw}); (C) intrinsic water use efficiency (iWUE); (D) specific leaf area ($\text{cm}^2 \text{g}^{-1}$); (E) relative chlorophyll content (SPAD values); and (F) leaf nitrogen content (%). Graphs show box plots of the 25th and 75th percentile, with a line indicating the median value. Each box plot shows the mean with a white circle, and gray dots showing individual observed residual data points ($n=10$), where letters within each panel indicate significant differences between genotypes.

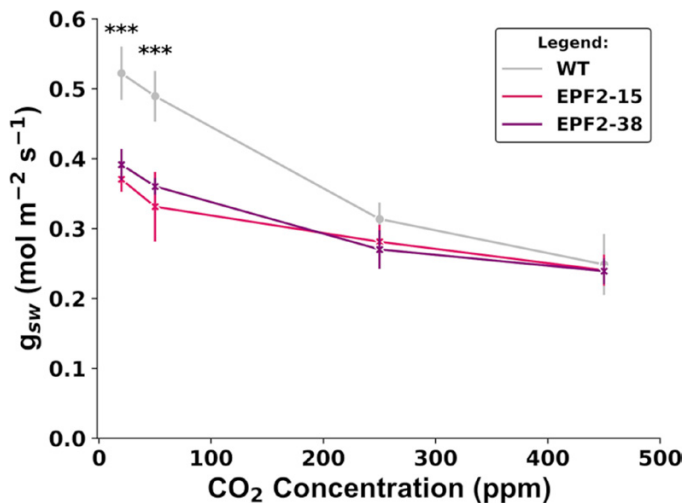


Fig. 6. Stomatal conductance of wild-type (WT) transgenic sugarcane overexpressing SbEPF2 (SbEPF2-15 and SbEPF2-38) at varying CO_2 concentrations. Error bars show the SE ($n=10$), with asterisks above each point indicating significant differences genotypes.

be assessed directly under a microscope (Karavolias *et al.*, 2023). Unfortunately, these techniques were ineffective in sugarcane because the pore apertures were too small to be reliably visible in imprints. These issues indicate that new methods are needed for assessing pore apertures across wide ranges of species and

environments. In the meantime, measurements of leaf gas exchange at very low $[\text{CO}_2]$ and saturating PPFD were used to assess g_{sw} when the stomatal aperture is close to its operational maximum. Under those conditions operating g_{sw} was 24–28% lower in SbEPF2-expressing lines than in the wild type (Fig. 6). This closely corresponds to the 24% and 30% reductions in g_{smax} predicted for the adaxial and abaxial surfaces, respectively, from stomatal anatomy (Fig. 4). This contrasts strongly with g_{sw} at ambient $[\text{CO}_2]$ where there was no difference in g_{sw} between low-SD and wild-type plants. Stomatal aperture is the only component of g_{sw} that can vary across the measurements of $[\text{CO}_2]$. Therefore, we conclude that a change in stomatal behavior is entirely responsible for fully compensating for the effect of reduced SD on g_{sw} .

At this time, when parallel studies engineering low SD through manipulation of EPFs and related genes have been done in ≥ 10 species, there is an opportunity to explore general principles through meta-analysis. We found that across three major plant functional types (C_3 dicots, C_3 monocots, and C_4 monocots), many studies observed that engineered reductions in SD did not reduce g_{sw} to an equivalent magnitude (Fig. 7). This suggests that the compensatory effects of larger stomatal complexes and/or altered stomatal aperture are probably more widespread than the previous experimental data on this trait suggest. Although this was especially true in the two monocot groups, the greater variability among experiments on C_3

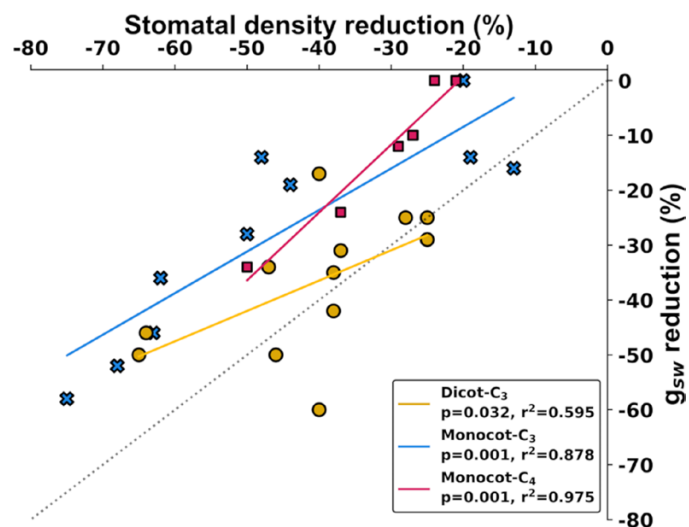


Fig. 7. Meta-analysis of the relationship between reduced stomatal density and lower stomatal conductance in transgenic species. The data show the SD and g_{sw} for individual transgenic events from publications listed in the Materials and methods. Shapes show C_3 dicot (yellow circles), C_3 monocot (blue crosses), and C_4 monocot (red squares) species. Trend lines were calculated using linear regression with the least-squares method. Lines show the 1–1 intercept (gray) and linear regression for C_3 dicots (yellow), C_3 monocots (blue), and C_4 monocots (red). The linear regression equations are for C_3 dicots: $y = 14.36 + 0.553x$; C_3 monocots $y = -6.694 + 0.757x$; and C_4 monocots $y = -25.427 + 1.237x$.

dicots means that further work is needed, ideally with multiple species grown side-by-side, to assess if differences among the functional groups are significant and consequential. In C_4 species, the x -axis intercept of the regression relationship suggests that SD must be reduced by >25% to start reducing g_{sw} . Beyond that threshold, for every 10% reduction in SD, there was a 12% reduction in g_{sw} . These data provide insight into the reduction of SD required to achieve a targeted reduction in g_{sw} . Fully understanding the relationship between SD and g_{sw} is especially significant when considering that increasingly substantial reductions in g_s will be desirable to maximize gains in iWUE of all functional types as atmospheric $[CO_2]$ continues to rise (Leakey *et al.*, 2019).

In conclusion, this report assessed the relationship between SD and g_{sw} in sugarcane engineered to have reduced SD. Although improvements in iWUE were not achieved, the study highlighted compensatory mechanisms that operate widely across species and functional groups to diminish the degree to which reductions in SD translate into reductions in g_{sw} . These findings are important since they highlight a fundamental knowledge gap in regulating leaf gas exchange, which can be addressed to advance our efforts to improve crop iWUE.

Supplementary data

The following supplementary data are available at [JXB online](#).

Fig. S1. Screening transgenic SbEPF2-expressing sugarcane events for low stomatal density.

Fig. S2. Expression of wild-type (WT) transgenic sugarcane overexpressing SbEPF2 (SbEPF2-15 and SbEPF2-38).

Fig. S3. Stomatal regions with more than one stomatal-containing file in wild-type (WT) transgenic sugarcane overexpressing SbEPF2 (SbEPF2-15).

Fig. S4. Epidermal patterning of bulliform cells in wild type (WT) and SbEPF2-expressing sugarcane (SbEPF2-15).

Fig. S5. Abaxial prickles regions with more than one prickle-containing file in wild-type (WT) transgenic sugarcane overexpressing SbEPF2 (SbEPF2-15).

Author contributions

DL: performed the research. BK, TEC, and FA generated recombinant DNA constructs. BK and FA carried out sugarcane transformation. AG and AL performed phenotyping on the plants. ADBL, FA, and DL contributed to the design of the research. All authors participated in writing and editing the manuscript.

Conflict of interest

The authors have no conflicts of interest to declare.

Funding

This material is based upon work supported by the DOE Center for Advanced Bioenergy and Bioproducts Innovation (U.S. Department of Energy, Office of Science, Biological and Environmental Research Program under Award Number DE-SC0018420). Any opinions, findings, conclusions, or recommendations expressed in this publication are those of the authors and do not necessarily reflect the views of the U.S. Department of Energy.

Data availability

All data supporting the findings of this study are included in the manuscript and supplementary material. Raw data supporting these figures is available through the University of Illinois Urbana-Champaign data bank under the title 'Greater aperture counteracts effects of reduced stomatal density on water use efficiency: a case study on sugarcane and meta-analysis' https://doi.org/10.13012/B2IDB-9701546_V1.

References

- Abrash E, Anleu Gil MX, Matos JL, Bergmann DC. 2018. Conservation and divergence of YODA MAPKKK function in regulation of grass epidermal patterning. *Development* **145**, dev165860.
- Al-Salman Y, Cano FJ, Pan L, Koller F, Piñeiro J, Jordan D, Ghannoum O. 2023. Anatomical drivers of stomatal conductance in sorghum lines with different leaf widths grown under different temperatures. *Plant, Cell & Environment* **46**, 2142–2158.

- Bergmann DC, Lukowitz W, Somerville CR.** 2004. Stomatal development and pattern controlled by a MAPKK kinase. *Science* **304**, 1494–1497.
- Bickford CP.** 2016. Ecophysiology of leaf trichomes. *Functional Plant Biology* **43**, 807–814.
- Budeguer F, Enrique R, Perera MF, Racedo J, Castagnaro AP, Noguera AS, Welin B.** 2021. Genetic transformation of sugarcane, current status and future prospects. *Frontiers in Plant Science* **12**, 768609.
- Büßis D, von Groll U, Fisahn J, Altmann T.** 2006. Stomatal aperture can compensate altered stomatal density in *Arabidopsis thaliana* at growth light conditions. *Functional Plant Biology* **33**, 1037–1043.
- Caine RS, Yin X, Sloan J, et al.** 2019. Rice with reduced stomatal density conserves water and has improved drought tolerance under future climate conditions. *New Phytologist* **221**, 371–384.
- Clemens M, Faralli M, Lagreze J, Bontempo L, Piazza S, Varotto C, Malnoy M, Oechel W, Rizzoli A, Dalla Costa L.** 2022. VvEPFL9-1 knockout via CRISPR/Cas9 reduces stomatal density in grapevine. *Frontiers in Plant Science* **13**, 878001.
- Des Marais DL, Auchincloss LC, Sukamtoh E, McKay JK, Logan T, Richards JH, Juenger TE.** 2014. Variation in MPK12 affects water use efficiency in *Arabidopsis* and reveals a pleiotropic link between guard cell size and ABA response. *Proceedings of the National Academy of Sciences, USA* **111**, 2836–2841.
- Dow GJ, Bergmann DC, Berry JA.** 2014. An integrated model of stomatal development and leaf physiology. *New Phytologist* **201**, 1218–1226.
- Dunn J, Hunt L, Afsharinafar M, Meselmani MA, Mitchell A, Howells R, Wallington E, Fleming AJ, Gray JE.** 2019. Reduced stomatal density in bread wheat leads to increased water-use efficiency. *Journal of Experimental Botany* **70**, 4737–4748.
- Farquhar GD, Sharkey TD.** 1982. Stomatal conductance and photosynthesis. *Annual Review of Plant Physiology* **33**, 317–345.
- Ferguson JN, Schmuker P, Dmitrieva A, Quach T, Zhang T, Ge Z, Nersesian N, Sato S, Clemente TE, Leakey ADB.** 2024. Reducing stomatal density by expression of a synthetic epidermal patterning factor increases leaf intrinsic water use efficiency and reduces plant water use in a C_4 crop. *Journal of Experimental Botany* **75**, <https://doi.org/10.1093/jxb/erae289>.
- Franks PJ, Doheny-Adams T W, Britton-Harper ZJ, Gray JE.** 2015. Increasing water-use efficiency directly through genetic manipulation of stomatal density. *New Phytologist* **207**, 188–195.
- Franks PJ, Drake PL, Beerling DJ.** 2009. Plasticity in maximum stomatal conductance constrained by negative correlation between stomatal size and density: an analysis using *Eucalyptus globulus*. *Plant, Cell & Environment* **32**, 1737–1748.
- Galdon-Armero J, Fullana-Pericas M, Mulet PA, Conesa MA, Martin C, Galmes J.** 2018. The ratio of trichomes to stomata is associated with water use efficiency in *Solanum lycopersicum* (tomato). *The Plant Journal* **96**, 607–619.
- Harrison EL, Arce Cubas L, Gray JE, Hepworth C.** 2020. The influence of stomatal morphology and distribution on photosynthetic gas exchange. *The Plant Journal* **101**, 768–779.
- Hepworth C, Doheny-Adams T, Hunt L, Cameron DD, Gray JE.** 2015. Manipulating stomatal density enhances drought tolerance without deleterious effect on nutrient uptake. *New Phytologist* **208**, 336–341.
- Hughes J, Hepworth C, Dutton C, Dunn JA, Hunt L, Stephens J, Waugh R, Cameron DD, Gray JE.** 2017. Reducing stomatal density in barley improves drought tolerance without impacting on yield. *Plant Physiology* **174**, 776–787.
- Hughes TE, Sedelnikova O, Thomas M, Langdale JA.** 2023. Mutations in NAKED-ENDOSPERM IDD genes reveal functional interactions with SCARECROW during leaf patterning in C_4 grasses. *PLoS Genetics* **19**, e1010715.
- Hunt L, Gray JE.** 2009. The signaling peptide EPF2 controls asymmetric cell divisions during stomatal development. *Current Biology* **19**, 864–869.
- Jiao Z, Han S, Li Z, Huang M, Niu M-X, Yu X, Liu C, Wang H-L, Yin W, Xia X.** 2022. PdEPFL6 reduces stomatal density to improve drought tolerance in poplar. *Industrial Crops and Products* **182**, 114873.
- Jolly E.** 2018. Pymer4: connecting R and Python for linear mixed modeling. *Journal of Open Source Software* **3**, 862.
- Karavolias NG, Patel-Tupper D, Seong K, et al.** 2023. Paralog editing tunes rice stomatal density to maintain photosynthesis and improve drought tolerance. *Plant Physiology* **192**, 1168–1182.
- Kellner J, Houska T, Manderscheid R, Weigel H-J, Breuer L, Kraft P.** 2019. Response of maize biomass and soil water fluxes on elevated CO_2 and drought—from field experiments to process-based simulations. *Global Change Biology* **25**, 2947–2957.
- Kong D, Pan X, Jing Y, et al.** 2021. ZmSPL10/14/26 are required for epidermal hair cell fate specification on maize leaf. *New Phytologist* **230**, 1533–1549.
- Lai LB, Nadeau JA, Lucas J, Lee E-K, Nakagawa T, Zhao L, Geisler M, Sack FD.** 2005. The *Arabidopsis* R2R3 MYB proteins FOUR LIPS and MYB88 restrict divisions late in the stomatal cell lineage. *The Plant Cell* **17**, 2754–2767.
- Leakey ADB, Ainsworth EA, Bernacchi CJ, Rogers A, Long SP, Ort DR.** 2009. Elevated CO_2 effects on plant carbon, nitrogen, and water relations: six important lessons from FACE. *Journal of Experimental Botany* **60**, 2859–2876.
- Leakey ADB, Ferguson JN, Pignon CP, Wu A, Jin Z, Hammer GL, Lobell DB.** 2019. Water use efficiency as a constraint and target for improving the resilience and productivity of C_3 and C_4 crops. *Annual Review of Plant Biology* **70**, 781–808.
- Li H, Yang Y, Wang H, et al.** 2021. The receptor-like kinase ERECTA confers improved water use efficiency and drought tolerance to poplar via modulating stomatal density. *International Journal of Molecular Sciences* **22**, 7245.
- Liu Y, Qin L, Han L, Xiang Y, Zhao D.** 2015. Overexpression of maize SDD1 (*ZmSDD1*) improves drought resistance in *Zea mays* L. by reducing stomatal density. *Plant Cell, Tissue and Organ Culture* **122**, 147–159.
- Long SP, Bernacchi CJ.** 2003. Gas exchange measurements, what can they tell us about the underlying limitations to photosynthesis? Procedures and sources of error. *Journal of Experimental Botany* **54**, 2393–2401.
- Markelz RJC, Strellner RS, Leakey ADB.** 2011. Impairment of C_4 photosynthesis by drought is exacerbated by limiting nitrogen and ameliorated by elevated $[CO_2]$ in maize. *Journal of Experimental Botany* **62**, 3235–3246.
- McKown KH, Bergmann DC.** 2020. Stomatal development in the grasses: lessons from models and crops (and crop models). *New Phytologist* **227**, 1636–1648.
- Mohammed U, Caine RS, Atkinson JA, Harrison EL, Wells D, Chater CC, Gray JE, Swarup R, Murchie EH.** 2019. Rice plants overexpressing OsEPF1 show reduced stomatal density and increased root cortical aerenchyma formation. *Scientific Reports* **9**, 5584.
- Nunes TDG, Berg LS, Slawinska MW, et al.** 2023. Regulation of hair cell and stomatal size by a hair cell-specific peroxidase in the grass *Brachypodium distachyon*. *Current Biology* **33**, 1844–1854.e6.
- Nunes TDG, Zhang D, Raissig MT.** 2020. Form, development and function of grass stomata. *The Plant Journal* **101**, 780–799.
- Pignon CP, Long SP.** 2020. Retrospective analysis of biochemical limitations to photosynthesis in 49 species: C_4 crops appear still adapted to pre-industrial atmospheric $[CO_2]$. *Plant, Cell & Environment* **43**, 2606–2622.
- Raissig MT, Abrash E, Bettadapur A, Vogel JP, Bergmann DC.** 2016. Grasses use an alternatively wired bHLH transcription factor network to establish stomatal identity. *Proceedings of the National Academy of Sciences, USA* **113**, 8326–8331.
- Raissig MT, Matos JL, Anleu Gil MX, et al.** 2017. Mobile MUTE specifies subsidiary cells to build physiologically improved grass stomata. *Science* **355**, 1215–1218.
- Roth-Nebelsick A, Hassiotou F, Veneklaas EJ.** 2009. Stomatal crypts have small effects on transpiration: a numerical model analysis. *Plant Physiology* **151**, 2018–2027.

- Schreuder MDJ, Brewer CA, Heine C.** 2001. Modelled influences of non-exchanging trichomes on leaf boundary layers and gas exchange. *Journal of Theoretical Biology* **210**, 23–32.
- Schuler ML, Sedelnikova OV, Walker BJ, Westhoff P, Langdale JA.** 2018. SHORTROOT-mediated increase in stomatal density has no impact on photosynthetic efficiency. *Plant Physiology* **176**, 757–772.
- Shen H, Zhong X, Zhao F, et al.** 2015. Overexpression of receptor-like kinase ERECTA improves thermotolerance in rice and tomato. *Nature Biotechnology* **33**, 996–1003.
- Simmons AR, Bergmann DC.** 2016. Transcriptional control of cell fate in the stomatal lineage. *Current Opinion in Plant Biology* **29**, 1–8.
- Sugano SS, Shimada T, Imai Y, Okawa K, Tamai A, Mori M, Hara-Nishimura I.** 2010. Stomagen positively regulates stomatal density in *Arabidopsis*. *Nature* **463**, 241–244.
- Taparia Y, Gallo M, Altpeter F.** 2012. Comparison of direct and indirect embryogenesis protocols, biolistic gene transfer and selection parameters for efficient genetic transformation of sugarcane. *Plant Cell, Tissue and Organ Culture* **111**, 131–141.
- Torii KU.** 2021. Stomatal development in the context of epidermal tissues. *Annals of Botany* **128**, 137–148.
- Wang C, Liu S, Dong Y, Zhao Y, Geng A, Xia X, Yin W.** 2016. PdEPF1 regulates water-use efficiency and drought tolerance by modulating stomatal density in poplar. *Plant Biotechnology Journal* **14**, 849–860.
- Wolz KJ, Wertin TM, Abordo M, Wang D, Leahey ADB.** 2017. Diversity in stomatal function is integral to modelling plant carbon and water fluxes. *Nature Ecology & Evolution* **1**, 1292–1298.
- Wu Z, Chen L, Yu Q, Zhou W, Gou X, Li J, Hou S.** 2019. Multiple transcriptional factors control stomata development in rice. *New Phytologist* **223**, 220–232.
- Xie J, Fernandes SB, Mayfield-Jones D, Erice G, Choi M, Lipka A E, Leahey ADB.** 2021. Optical topometry and machine learning to rapidly phenotype stomatal patterning traits for maize QTL mapping. *Plant Physiology* **187**, 1462–1480.
- Yoo CY, Pence HE, Hasegawa PM, Mickelbart MV.** 2009. Regulation of transpiration to improve crop water use. *Critical Reviews in Plant Sciences* **28**, 410–431.
- Zhao P-X, Miao Z-Q, Zhang J, Chen S-Y, Liu Q-Q, Xiang C-B.** 2020. *Arabidopsis* MADS-box factor AGL16 negatively regulates drought resistance via stomatal density and stomatal movement. *Journal of Experimental Botany* **71**, 6092–6106.
- Zhu Z, Xu X, Cao B, Chen C, Chen Q, Xiang C, Chen G, Lei J.** 2015. Pyramiding of AtEDT1/HDG11 and Cry2Aa2 into pepper (*Capsicum annuum* L.) enhances drought tolerance and insect resistance without yield decrease. *Plant Cell, Tissue and Organ Culture* **120**, 919–932.
- Zoulias N, Harrison EL, Casson SA, Gray JE.** 2018. Molecular control of stomatal development. *The Biochemical Journal* **475**, 441–454.